ChemComm

COMMUNICATION

View Article Online
View Journal | View Issue

Cite this: *Chem. Commun.*, 2022, **58**, 13791

Received 20th October 2022,
Accepted 17th November 2022

DOI: 10.1039/d2cc05697f

rsc.li/chemcomm

A dinoflagellate-inspired mechanochromic film for fast and reversible information encryption and display†

Depeng Liu,[ab] Longqiang Li,[ac] Guangqiang Yin *[ab] and Tao Chen *[ab]

Inspired by dinoflagellates, we developed a flexible film consisting of spiropyran-based soft polyacrylate and $Zn(OTf)_2$. The open-ring form of spiropyran coordinated with $Zn(OTf)_2$ under stretching to produce a visible fluorescent color change from colorless to yellow. The potential of this film was demonstrated for fast and reversible information encryption and decryption.

In nature, cephalopods (squid, cuttlefish, octopus, *etc.*) and chameleons can change their colors upon external stimulation to hide from predators or communicate with their rivals and mates. Inspired by these phenomena, a variety of materials and devices that undergo color changes flexibly based on photochromism,[1,2] thermochromism,[3,4] solvatochromism,[5,6] mechanochromism,[7,8] electrochromism,[9,10] or magnetochromism[11] according to different external stimuli have been developed. In particular, compared to other types of discoloration, mechanochromism is quite distinctive because external equipment (*i.e.*, used for optical or electrical excitation) is not required. Therefore, mechanochromic polymers or devices with remarkable discoloration ability under mechanical stimulation have certain advantages, making them attractive for a wide range of applications in stress/strain sensing,[12,13] structural health monitoring,[14,15] stretchable electronic display,[16,17] information encryption applications,[18] *etc.*

Interestingly, one of the characteristic features of many marine dinoflagellates is their bioluminescence, which is usually triggered by fluid shear or mechanical force (*i.e.*, breaking waves). The mechanism of this miraculous phenomenon is that changes in the intracellular calcium levels of dinoflagellates produce an action potential, opening voltage-gated proton channels in the membranes of organelles called scintillons, lowering the pH within them[19,20] and then leading to the oxidation of the protein luciferin catalyzed by luciferase (Scheme 1a).

Spiropyrans (SP), as a well-known class of reversible photoswitch molecules, have been widely researched and applied in many fields over the past few decades. In addition to UV and visible light, when SP molecules are appropriately linked to a polymer backbone, merocyanine (MC) isomerization can also be triggered by mechanical force. Due to the zwitterionic nature of the MC molecule, its fluorescence emission could be significantly affected by the surrounding media. It has been reported that a few specific metal ions can bind to MC through the negatively charged phenolate group of the zwitterionic form.[21] As a result, notable changes occur in its absorption or fluorescence properties.[22,23] Therefore, unlike many existing materials and devices[24–29] that have the ability to respond to light,

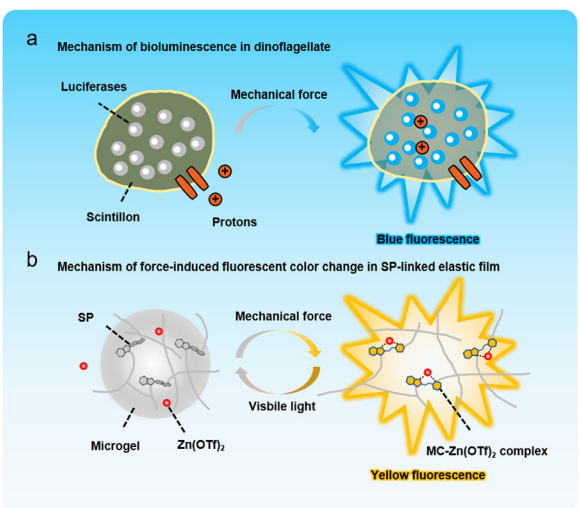

Scheme 1 (a) The mechanism of bioluminescence in dinoflagellates. (b) Dinoflagellate-inspired SP-linked elastic film and the mechanism of its force-induced fluorescent color change.

[a] *Key Laboratory of Marine Materials and Related Technologies, Zhejiang Key Laboratory of Marine Materials and Protective Technologies, Ningbo Institute of Material Technology and Engineering, Chinese Academy of Sciences, Ningbo 315201, China. E-mail: yinguangqiang@nimte.ac.cn, tao.chen@nimte.ac.cn*
[b] *School of Chemical Sciences, University of Chinese Academy of Sciences, Beijing 100049, China*
[c] *College of Material Sciences and Opto-Electronic Technology, University of Chinese Academy of Sciences, Beijing 100049, China*

† Electronic supplementary information (ESI) available: Experimental details and Fig. S1–S7. See DOI: https://doi.org/10.1039/d2cc05697f

electricity, and temperature, this property of SP is expected to construct a novel mechanochromic material for information encryption and display.

Herein, inspired by the force-induced bioluminescence of dinoflagellates, we develop a novel encryption mechanochromic strategy *via* the reversible coordinative interaction in MC-$Zn(OTf)_2$ complexes. We utilize the different fluorescent features between MC and MC-$Zn(OTf)_2$ complexes to design and prepare an elastic film that exhibits mechanical force induced fluorescent color transformation (Scheme 1b). The covert–overt encryption and display techniques are facilely and rapidly transformed in the film under mechanical stimuli. Image information can be easily patterned on the film by ion transfer printing. Interestingly, these patterns are invisible under sunlight, as well as 365 nm UV light. However, clear patterns can be observed under mechanical force on demand, while they subsequently disappeared under visible light within several minutes. This film features practical, simple, convenient, and secure characteristics, thus enabling potential applications in information encryption and display.

The elastic film with mechanical force induced fluorescent color transformation was first prepared by visible light-initiated emulsion polymerization (Fig. S1, ESI†). Herein, hydrophobic ethyl acrylate (EA) and di(ethylene glycol)methyl ether acrylate (DEGMEA) monomers play a vital role in the preparation of elastic films. These two monomers were selected not only to incorporate highly hydrophobic SP into the polymer network in microgels, but also to obtain the final films with good flexibility and elasticity because of their low glass transition temperature (T_g). Hydrophilic acrylamide (AM) monomer was also introduced into the system to crosslink with each microgel. By this means, in the elastic poly(EA-DEGMEA-SP/AAm) film, mechanical force was intensively transferred to the SP-crosslinked polymer chains inside microgels while being less dispersed to other contrast networks or to align polymer chains, resulting in the cleavage of the linkages of SP mechanophores, favoring the activation of SP.[30]

Considering the effect of solution pH on SP to MC isomerization,[31] ethanol solutions were used for solubilizing the metal ions and maintaining a constant pH. In order to explore and compare the effect of different divalent metal salts on the fluorescence changes of films before and after stretching, we prepared an ethanol solution of Zn^{2+}, Ca^{2+}, Mg^{2+}, Sn^{2+}, Ni^{2+}, Co^{2+}, and Cu^{2+} chloride salts at a concentration of 0.01 M to soak the films. It was reported that the counterions can also influence the absorption spectra of the MC-M^{2+} complex,[32] and thus $Zn(CH_3COO)_2$ and $Zn(OTf)_2$ were chosen as well. When using Ca^{2+}, Mg^{2+}, Sn^{2+}, Ni^{2+}, Co^{2+} and Cu^{2+} chloride salts, there was no significant fluorescence color change in each group before and after stretching (Fig. S2 and S3, ESI†). Only the film treated with $Zn(OTf)_2$ solution exhibited a noticeable fluorescent color change after stretching under 365 nm UV light. In striking contrast, no obvious fluorescence change can be observed upon treating with $ZnCl_2$ and $Zn(CH_3COO)_2$ (Fig. 1a).

To gain more insights into the effect of different zinc salts on the fluorescence properties of films, we measured the fluorescence spectra of three films before and after stretching. There was almost no change in the fluorescence spectra of poly(EA-DEGMEA-SP/AAm)@$ZnCl_2$ before and after stretching.

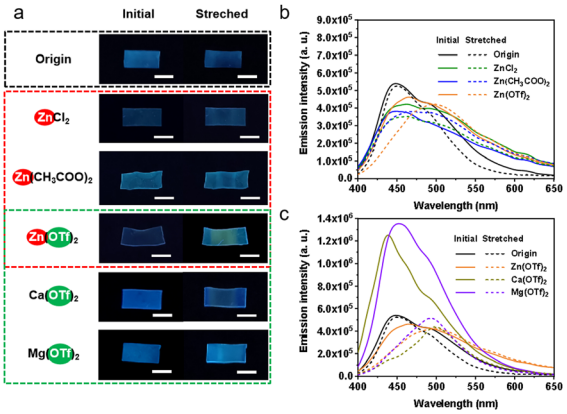

Fig. 1 (a) Stretch-induced fluorescence photographs of elastic films treated with different metal salts before and after stretching. Photographs were taken under 365 nm UV light. Scale bar: 5 mm. (b) The fluorescence spectra of the films treated with $ZnCl_2$, $Zn(CH_3COO)_2$ and $Zn(OTf)_2$ before and after stretching. (c) The fluorescence spectra of the films treated with $Zn(OTf)_2$, $Ca(OTf)_2$ and $Mg(OTf)_2$ before and after stretching.

Also, poly(EA-DEGMEA-SP/AAm)@$Zn(CH_3COO)_2$ displayed only a small shift from 450 to 468 nm upon stretching. Surprisingly, a significant red-shift of the maximum emission wavelength of poly(EA-DEGMEA-SP/AAm)@$Zn(OTf)_2$ from the initial value of 466 to 498 nm was observed after stretching (Fig. 1b). These results were consistent with the optical photographs of the three films under 365 nm UV light (Fig. 1a). The UV-Vis absorption spectra of poly(EA-DEGMEA-SP/AAm) films with or without $Zn(OTf)_2$ were also measured which showed slight difference after stretching (Fig. S4, ESI†). Therefore, the emission of MC-$Zn(OTf)_2$ was different from that of the MC form, and there might be energy transfer between them due to the matchable emission spectrum of MC-Zn^{2+} and the absorption spectrum of MC.[34] To further examine the effects of OTf ions on mechanochromism, other triflates, such as $Ca(OTf)_2$ and $Mg(OTf)_2$, were used to prepare the poly(EA-DEGMEA-SP/AAm)@$Ca(OTf)_2$ and poly(EA-DEGMEA-SP/AAm)@$Mg(OTf)_2$ films. Interestingly, the fluorescence spectra of poly(EA-DEGMEA-SP/AAm) films with $Ca(OTf)_2$ and $Mg(OTf)_2$ also showed a large red-shift of the maximum emission wavelength from 438 to 499 nm and 452 to 494 nm, respectively, after stretching (Fig. 1c). However, the fluorescence discoloration of these two films is relatively difficult to be observed directly due to the lack of a high degree of visual contrast (Fig. 1a). Therefore, in our experiments, $Zn(OTf)_2$ is one of the more desirable choices in the construction of pattern information. Based on these results, we speculate that the force-induced fluorescent color change within the poly(EA-DEGMEA-SP/AAm)@$Zn(OTf)_2$ may be related to the synergistic interaction between Zn cations and OTf anions with MC. Besides, the concentration of the metal salt also has a great influence on the fluorescence properties of the films. The maximum emission wavelength of the films treated with 10^{-4} and 10^{-3} M $Zn(OTf)_2$ ethanol solution remains almost unchanged before and after stretching. When the concentration increased to 0.1 M, the film shows a maximum emission wavelength of 508 nm before stretching (Fig. S5, ESI†). Therefore, the optimal concentration

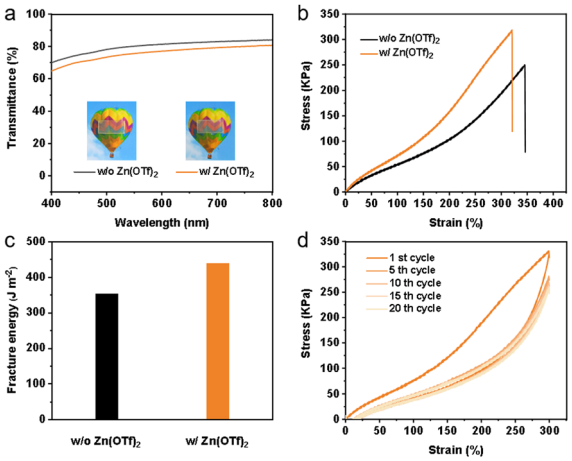

Fig. 2 (a) The transmittance of the poly(EA-DEGMEA-SP/AAm) films with or without $Zn(OTf)_2$ in the visible wavelength range. Inset: Photographs of the films. (b) Stress–strain curves of poly(EA-DEGMEA-SP/AAm) and poly(EA-DEGMEA-SP/AAm)@$Zn(OTf)_2$ films. (c) Fracture energy of the poly(EA-DEGMEA-SP/AAm) film with or without $Zn(OTf)_2$. (d) Cyclic stress–strain curves for the 1st, 5th, 10th, 15th and 20th cycles of poly(EA-DEGMEA-SP/AAm)@$Zn(OTf)_2$ films.

of $Zn(OTf)_2$ is 0.01 M and used in the subsequent study. Moreover, the absolute fluorescence quantum efficiency of the poly(EA-DEGMEA-SP/AAm)@$Zn(OTf)_2$ film before and after stretching is 2.25% and 3.05%, respectively, as determined on a QE-2100 quantum efficiency measurement system.

The film has good optical transparency, making it possible to be used as a useful platform for information display. The transmittance of these films can reach up to around 80% with or without $Zn(OTf)_2$ (Fig. 2a). It has been demonstrated in previous reports that the mechanoactivation of the incorporated mechanophores greatly depends on the mechanical properties of materials and a higher strength favors the activation of spiropyrans.[33] To evaluate the effect of $Zn(OTf)_2$ on the mechanical properties of the poly(EA-DEGMEA-SP/AAm)@$Zn(OTf)_2$ film, the mechanical tests were carried out at room temperature. The typical stress–strain curves of the poly(EA-DEGMEA-SP/AAm)@$Zn(OTf)_2$ film indicated excellent mechanical properties and a tensile strength of 320 KPa was achieved at a fracture strain of 320%. Besides, a pronounced enhancement of mechanical properties occurred when $Zn(OTf)_2$ was added, which was attributed to the continuous formation of MC-Zn^{2+} complexes with physical cross-linking during stretching (Fig. 2b). The fracture energy of the poly(EA-DEGMEA-SP/AAm)@$Zn(OTf)_2$ film was up to 439 J m^{-2}, which was 1.24 times higher than that of the poly(EA-DEGMEA-SP/AAm) film ($\approx$ 354 J m^{-2}) (Fig. 2c).

The poly(EA-DEGMEA-SP/AAm)@$Zn(OTf)_2$ film showed a large hysteresis loop and dissipated energy in the first loading–unloading cycle at a strain of 300%, as compared to a slightly smaller one of the poly(EA-DEGMEA-SP/AAm) film without $Zn(OTf)_2$ (Fig. 2d and Fig. S6, ESI†). This indicated that the force-induced conversion from SP to MC in the presence of $Zn(OTf)_2$, *i.e.*, coordination between MC and $Zn(OTf)_2$, contributed largely to high dissipated energies and toughness of SP-conjugated films. In the immediate second cycle, hysteresis loops became much smaller for both SP-linked films with or without $Zn(OTf)_2$, indicating that the films can be recovered rapidly. In total, 20 cycles of loading–unloading were tested. Starting with the second cycle, each cycle with an approximate situation (Fig. S6, ESI†), revealing stable, high toughness and low hysteresis of the film. The stress relaxation of films was also measured in λ = 1, 2, and 3. The films exhibited almost no relaxation in small deformation (λ = 1) and only relaxed no more than 30% stress at λ = 3 (Fig. S7, ESI†). Therefore, the film exhibited good elasticity and kept the network intact under consecutive, highly deformed loading–unloading processes to provide stable and repeatable mechanical properties.

It is important that the mild binding strength of MC to metal ions is essential for the binding and release: if the interaction energy was too weak, neither isomer of the switch would bind metal ions; if it was too strong, the binding would be irreversible.[35] So we also tested the fluorescence spectra of the stretched poly(EA-DEGMEA-SP/AAm)@$Zn(OTf)_2$ film at intervals after being irradiated with visible light (0.4 W m^{-2}) to evaluate the recovery behavior. With the increase of exposure time, the maximum fluorescence emission peak was gradually blue-shifted. It returned to the initial state completely after nine minutes (Fig. 3a). This result manifested that the Zn^{2+} in MC-Zn^{2+} complexes can be released by visible light irradiation. The Commission Internationale de L'Eclairage (CIE) coordinates of the fluorescence of the stretched poly(EA-DEGMEA-SP/AAm) film before and after light irradiation are (0.28, 0.40) and (0.20, 0.26), corresponding to yellowish and cyan emissions, respectively (Fig. 3b). Rapid deactivation of the MC–M^{2+} complexes is induced by exposing the films to intense visible light, enabling multiple activation/deactivation cycles within minutes. These results prove that force-triggered MC–Zn^{2+} coordination is reversible and dynamic. It is worth noting that the reversibility of this process is due to both the intrinsic reversibility of the SP-to-MC isomerization and the dynamic nature of the MC–Zn^{2+} coordinate bonds.[36] Based on the above results, the reversible interactions between SP and $Zn(OTf)_2$ under stretching and visible light are depicted in Fig. 3c.

The accessibility and reversibility of the color-switchable film are like two different accesses to a lock. Only the minority who holds the key can unlock it and encrypt the information. Different from common light response and other stimulus response information display strategies, the key here is mechanical force. The designed patterns of a crab and "SOS" are composed of the yellow part, which were printed with $Zn(OTf)_2$ ink (Fig. 4a). The crab pattern printed with $Zn(OTf)_2$ ink is invisible under 365 nm UV light, while it displays yellow emission immediately after being decoded by mechanical force. The film with the other pattern, *i.e.* the "SOS" pattern, shows the same properties. The subsequent treatment can mask the message again when exposed to visible light for several minutes, thus making the decoding process trackless (Fig. 4b). More importantly, even after several decoding/encryption cycles, the crab and SOS patterns still can be identified, so the information can be decoded and re-encrypted multiple times.

In summary, we presented an effective strategy to realize efficient information encryption based on the fast and reversible mechanochromic behavior of MC-$Zn(OTf)_2$ complexes in a polymer elastic film. The significant spectral difference between MC and MC-$Zn(OTf)_2$ complexes was used to achieve encryption mechanochromism. In addition, the prepared polymer elastic film had good

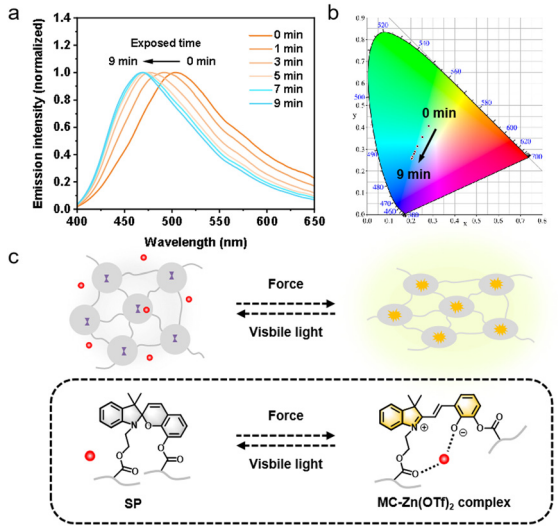

Fig. 3 (a) The recovery performance of the poly(EA-DEGMEA-SP/AAm)@Zn(OTf)$_2$ elastic film under visible light. (b) The CIE coordinates of the poly(EA-DEGMEA-SP/AAm)@Zn(OTf)$_2$ elastic film during the color recovery under visible light. (c) Schematic of the interactions between SP and Zn(OTf)$_2$ under stretching and visible light.

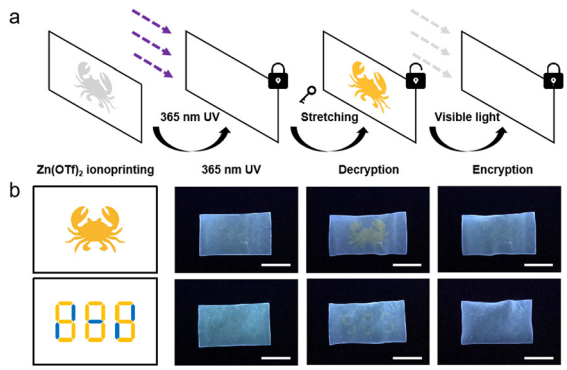

Fig. 4 Hidden information patterning and force-induced information encryption and display. (a) Schematic of the reversible information encryption and decryption process. (b) Photographs of the concealed "crab" and "SOS" patterns within the elastic film were revealed after stretching and re-disappearance after being irradiated with visible light. Scale bar: 1 cm.

tensile repeatability to ensure multiple cycles of encrypted information and display. Overall, it is anticipated that this design principle can be extended to fabricate stress-induced response devices for advanced encryption mechanochromism.

We greatly acknowledge the financial support from the National Key R&D Program of China (2022YFB3204301), National Natural Science Foundation of China (22205249), China Postdoctoral Science Foundation (2021TQ0341), Ningbo Natural Science Foundation (2021J203), and the Foundation of the Director of NIMTE (2021SZKY0305).

Conflicts of interest

There are no conflicts to declare.

Notes and references

1 A. Abdollahi, H. Roghani-Mamaqani and B. Razavi, *Prog. Polym. Sci.*, 2019, **98**, 101149.
2 A. Abdollahi, H. Roghani-Mamaqani, B. Razavi and M. Salami-Kalajahi, *ACS Nano*, 2020, **14**, 14417–14492.
3 A. Seeboth, D. Lötzsch, R. Ruhmann and O. Muehling, *Chem. Rev.*, 2014, **114**, 3037–3068.
4 Y. Cui, Y. Ke, C. Liu, Z. Chen, N. Wang, L. Zhang, Y. Zhou, S. Wang, Y. Gao and Y. Long, *Joule*, 2018, **2**, 1707–1746.
5 E. Li, K. Jie, M. Liu, X. Sheng, W. Zhu and F. Huang, *Chem. Soc. Rev.*, 2020, **49**, 1517–1544.
6 A. Steinegger, O. S. Wolfbeis and S. M. Borisov, *Chem. Rev.*, 2020, **120**, 12357–12489.
7 Y. Chen, G. Mellot, D. van Luijk, C. Creton and R. P. Sijbesma, *Chem. Soc. Rev.*, 2021, **50**, 4100–4140.
8 T. Han, L. Liu, D. Wang, J. Yang and B. Z. Tang, *Macromol. Rapid Commun.*, 2021, **42**, 2000311.
9 C. Gu, A.-B. Jia, Y.-M. Zhang and S. X.-A. Zhang, *Chem. Rev.*, 2022, **122**, 14679–14721.
10 M. Lahav and M. E. van der Boom, *Adv. Mater.*, 2018, **30**, 1706641.
11 W. Wang, X. Fan, F. Li, J. Qiu, M. M. Umair, W. Ren, B. Ju, S. Zhang and B. Tang, *Adv. Opt. Mater.*, 2018, **6**, 1701093.
12 M. Wu, Y. Li, W. Yuan, G. De Bo, Y. Cao and Y. Chen, *J. Am. Chem. Soc.*, 2022, **144**, 17120–17128.
13 M. Raisch, D. Genovese, N. Zaccheroni, S. B. Schmidt, M. L. Focarete, M. Sommer and C. Gualandi, *Adv. Mater.*, 2018, **30**, 1802813.
14 W. Li, C. C. Matthews, K. Yang, M. T. Odarczenko, S. R. White and N. R. Sottos, *Adv. Mater.*, 2016, **28**, 2189–2194.
15 C. Calvino, A. Guha, C. Weder and S. Schrettl, *Adv. Mater.*, 2018, **30**, 1704603.
16 M. H. Barbee, K. Mondal, J. Z. Deng, V. Bharambe, T. V. Neumann, J. J. Adams, N. Boechler, M. D. Dickey and S. L. Craig, *ACS Appl. Mater. Interfaces*, 2018, **10**, 29918–29924.
17 J. Park, Y. Lee, M. H. Barbee, S. Cho, S. Cho, R. Shanker, J. Kim, J. Myoung, M. P. Kim, C. Baig, S. L. Craig and H. Ko, *Adv. Mater.*, 2019, **31**, 1808148.
18 S. Zeng, D. Zhang, W. Huang, Z. Wang, S. G. Freire, X. Yu, A. T. Smith, E. Y. Huang, H. Nguon and L. Sun, *Nat. Commun.*, 2016, **7**, 11802.
19 M. Fogel and J. W. Hastings, *Proc. Natl. Acad. Sci. U. S. A.*, 1972, **69**, 690–693.
20 M. Jalaal, N. Schramma, A. Dode, H. de Maleprade, C. Raufaste and R. E. Goldstein, *Phys. Rev. Lett.*, 2020, **125**, 028102.
21 A. S. Terpstra, W. Y. Hamad and M. J. MacLachlan, *Adv. Funct. Mater.*, 2017, **27**, 1703346.
22 K. H. Fries, G. R. Sheppard, J. A. Bilbrey and J. Locklin, *Polym. Chem.*, 2014, **5**, 2094–2102.
23 M. Baldrighi, G. Locatelli, J. Desper, C. B. Aakeröy and S. Giordani, *Chem. – Eur. J.*, 2016, **22**, 13976–13984.
24 X. Le, H. Shang, H. Yan, J. Zhang, W. Lu, M. Liu, L. Wang, G. Lu, Q. Xue and T. Chen, *Angew. Chem., Int. Ed.*, 2021, **60**, 3640–3646.
25 H. Shang, X. Le, Y. Sun, F. Shan, S. Wu, Y. Zheng, D. Li, D. Guo, Q. Liu and T. Chen, *Adv. Opt. Mater.*, 2022, **10**, 2200608.
26 H. Lu, B. Wu, X. Le, W. Lu, Q. Yang, Q. Liu, J. Zhang and T. Chen, *Adv. Funct. Mater.*, 2022, **55**, 2206912.
27 Y. Sun, X. Le, S. Zhou and T. Chen, *Adv. Mater.*, 2022, **34**, 2201262.
28 W. Lu, M. Si, X. Le and T. Chen, *Acc. Chem. Res.*, 2022, **55**, 2291–2303.
29 J. Wei, L. Li, R. Li, Q. Liu, Z. Yan and T. Chen, *Int. J. Smart Nano Mater.*, 2022, 1–14.
30 H. Chen, F. Yang, Q. Chen and J. Zheng, *Adv. Mater.*, 2017, **29**, 1606900.
31 C. Li, A. Iscen, L. C. Palmer, G. C. Schatz and S. I. Stupp, *J. Am. Chem. Soc.*, 2020, **142**, 8447–8453.
32 K. H. Fries, J. D. Driskell, G. R. Sheppard and J. Locklin, *Langmuir*, 2011, **27**, 12253–12260.
33 B. A. Beiermann, S. L. B. Kramer, P. A. May, J. S. Moore, S. R. White and N. R. Sottos, *Adv. Funct. Mater.*, 2014, **24**, 1529–1537.
34 Y. Shi, J. Han, X. Jin, W. Miao, Y. Zhang and P. Duan, *Adv. Sci.*, 2022, **9**, 2201565.
35 A. Radu, R. Byrne, N. Alhashimy, M. Fusaro, S. Scarmagnani and D. Diamond, *J. Photochem. Photobiol., A*, 2009, **206**, 109–115.
36 E. Epstein, T. A. Kim, R. H. Kollarigowda, N. R. Sottos and P. V. Braun, *Chem. Mater.*, 2020, **32**, 3869–3878.